Coupled TLM-Thermal Analysis in the Time Domain

Wei Liu, Poman P.M. So and Wolfgang J.R. Hoefer

Computational Electromagnetics Research Laboratory
Department of Electrical and Computer Engineering
University of Victoria, Victoria, V8W 3P6, Canada

http://www.wjrh.ece.uvic.ca

***Abstract* — A coupled time domain TLM-thermal analysis technique will be presented in this paper. It is a hybrid combination of algorithms comprising TLM, FDTD and ray optical algorithms for evaluating the transient thermal behavior of objects placed inside a cavity or waveguide. Electromagnetic fields are calculated using a GSCN 3D TLM algorithm. We have developed the analysis procedure primarily for evaluating power handling capability of waveguide and microstrip structures. Nevertheless, this procedure can be applied to general microwave heating problems.**

I. Introduction

A coupled TLM-thermal algorithm has been implemented for modeling the thermal behavior of metallic and dielectric objects in guiding and resonating microwave structures. Electromagnetic fields are calculated using the generalized symmetrical condensed node TLM algorithm [1]; the power dissipated in both metallic boundaries and dielectric objects are used as the source of power distribution for the thermal calculation. Heat conduction is modeled by an explicit FDTD scheme; heat radiation exchange between the surfaces inside the waveguide is modeled using a ray optical algorithm to determine the line-of-sight interaction between the inner surfaces, [2] and [3]. The algorithm has been used to analyze a single-mode microwave oven with a polyvinyl chloride (PVC) sample in its center, and the numerical results are shown at the end of this paper.

II. Calculation of EM Power with TLM Analysis

According to Poynting's theorem, the time-average power dissipated in the volume V due to conductivity, dielectric, and magnetic losses is defined as:

$$P_{EM} = \frac{\sigma}{2}\int_V \left|\bar{E}\right|^2 dv + \frac{\omega}{2}\int_V (\varepsilon''\left|\bar{E}\right|^2 + \mu''\left|\bar{H}\right|^2)dv \qquad (1)$$

Where σ is the electric conductivity, ω is angular frequency, $\bar{E}$ and $\bar{H}$ are the total electric and magnetic fields in the volume V and, ε'' and μ'' are the imaginary parts of the complex permittivity and permeability, respectively.

The calculation of the power absorbed by a good conductor can be simplified by determining the tangential magnetic field at the surface of the conductor, [5]:

$$P_{EM} = \frac{R_s}{2}\int_{S_0} \left|\bar{H}\right|^2 ds \qquad (2)$$

Where $\bar{H}$ is the tangential magnetic field at the conductor surface S_0. This field is obtained from the TLM mesh. R_S is the surface resistivity of the conductor given by:

$$R_s = \mathrm{Re}(\eta) = \mathrm{Re}\left[(1+j)\sqrt{\frac{\omega\mu}{2\sigma}}\right] = \sqrt{\frac{\omega\mu}{2\sigma}} \qquad (3)$$

III. Overview of Thermal Computation

Once the average electromagnetic input power to the volume of interest is obtained, computation of heat transfer can be performed by following the procedures outlined in [2] and [3]. Three mechanisms of heat transfer are included in our thermal algorithm, namely conduction, convection and radiation. The algorithm does not consider forced cooling, i.e. only free convection is considered. Furthermore, the outer surfaces of the vertical waveguide walls are assumed smooth so that the airflow along these walls is laminar. Finally, convection inside the waveguide is negligible due to the small dimensions of the structure.

Heat conduction is modeled with a finite difference scheme assuming the temperature inside a FDTD cell to be homogeneous. A uniform mesh is used for the calculation of conduction heat flux. The heat conduction is computed in such a way that for every single cell the power flux in all the six directions is computed individually and then summed up to yield the total heat power flux through that cell. The power flux in positive *x*-direction is:

0-7803-6540-2/01/$10.00 (C) 2001 IEEE

$$PXP_{i,j,k} = \frac{2\Delta l k_{i,j,k} k_{i+1.j,k}}{k_{i,j,k} + k_{i+1.j,k}} (T_{i,j,k} - T_{i+1,j,k}) \quad (4)$$

The power flux in negative *x*-direction is:

$$PXN_{i,j,k} = \frac{2\Delta l k_{i-1,j,k} k_{i,j,k}}{k_{i-1,j,k} + k_{i,j,k}} (T_{i-1,j,k} - T_{i,j,k}) \quad (5)$$

where Δl and k denote the cell size and the temperature-dependent thermal conductivity of the materials, respectively. Similar equations can be written for the power flux in the *y*- and *z*-directions, [2]. The total heat conduction power flux $P_{i,j,k}^{COND}$ is then obtained as:

$$P_{i,j,k}^{COND} = PXN_{i,j,k} - PXP_{i,j,k} + PYN_{i,j,k} - PYP_{i,j,k} + PZN_{i,j,k} - PZP_{i,j,k} \quad (6)$$

Heat convection power flux is calculated as:

$$P_{i,j,k}^{CVEC} = h_{i,j,k} (T_{i,j,k} - T_{fluid}) \quad (7)$$

where $h_{i,j,k}$ is the heat transfer coefficient at cell$_{i,j,k}$, [2].

Heat exchanges due to radiation include radiation to free space as well as heat transfers between the specific cell and all the visible surface cells:

$$P_{i,j,k}^{FREERAD} = \varepsilon \sigma T_{i,j,k}{}^4 \Delta l^2 \quad (8)$$

where ε is the emissivity of the surface and σ is Stefan-Boltzman constant.

$$P_{i,j,k}^{EXRAD} = \sum_{\substack{Visible \\ Surfaces}} \left(\Phi_{(i,j,k)(l,m,n)} - \Phi_{(l,m,n)(i,j,k)} \right) \quad (9)$$

where

$$\Phi_{(i,j,k)(l,m,n)} = \varepsilon_{i,j,k} \alpha_{l,m,n} F_{i,j,k,l,m,n} \sigma T_{i,j,k}^4 \quad (10)$$

$$F_{ss'} = \frac{1}{\pi A_s} \int_{A_s} \int_{A_{s'}} \frac{\cos(\theta_s)\cos(\theta_{s'})}{r^2} dA_s dA_{s'} \quad (11)$$

Here α is the absorptivity of the surface, which is usually equal to the emissivity of that surface, and F is the shape factor determined by geometry only. This coefficient is defined as the part of energy transmitted from one cell surface s to another cell surface s', divided by the total energy emitted by the surface s. θ and r describe the relative positions of the surfaces s and s'.

Once all the above power fluxes are calculated, the temperature can be updated as follows:

$$T_{i,j,k}^{n+1} = T_{i,j,k}^{n} + \frac{\Delta t}{m_{i,j,k} c_{i,j,k}} P_{i,j,k}^{TOTAL} = T_{i,j,k}^{n} + \frac{\Delta t}{\Delta l^3 \rho_{i,j,k} c_{i,j,k}} \begin{pmatrix} P_{i,j,k}^{EM} + P_{i,j,k}^{COND} - P_{i,j,k}^{CVEC} - \\ P_{i,j,k}^{FREERAD} - P_{i,j,k}^{EXRAD} \end{pmatrix} \quad (12)$$

where Δt is the thermal calculation time step, ρ is the density, and c is the specific heat constant. Furthermore, $P_{i,j,k}^{EXRAD}$ only applies to inner surface cells of the structure, and $P_{i,j,k}^{CONV}$ and $P_{i,j,k}^{FREERAD}$ only apply to outer surface cells of the structure. When the total power flux entering the structure equals to the total power flux emerging from it, the temperature reaches a steady state.

IV. Coupled TLM-Thermal Implementation

The thermal and electric conductivities of most materials are slightly dependent upon the temperature. Even though the assumption of uniform and constant thermal and electric conductivity is generally acceptable for problems involving small temperature difference, some situations are encountered in which the variation in conductivities with temperature cannot be neglected. The temperature dependence of thermal conductivity is usually expressed as:

$$k(T) = k_0 (1 + \beta T) \quad (13)$$

where β in $1/^oK$ is known as the temperature coefficient of the thermal conductivity and is widely available in the literature. The temperature dependence of the electric conductivity is usually expressed as:

$$\sigma(T) = \frac{1}{\rho(T)} = \frac{1}{\rho(T_0)(1 + \alpha(T - T_0))} \quad (14)$$

where σ is the electric conductivity, ρ is the resistivity, T is the absolute temperature in ^oK, T_0 is the reference temperature (usually room temperature), and α is the temperature coefficient describing the relation between resistivity and temperature. $\rho(T_0)$ and α are available from material property tables in the literature.

The surface impedance Z_S and the reflection coefficient Γ must be determined to obtain the EM power absorbed by the objects. Z_S and Γ are also temperature dependent as they are related to the electric conductivity by

$$Z_s = \frac{1}{\sigma(T)\delta(T)} \tag{15}$$

and

$$\Gamma = \frac{Z_s - Z_0}{Z_s + Z_0} \tag{16}$$

where Z_0 is the characteristic impedance; $\sigma(T)$ and $\delta(T)$ are the temperature-dependent conductivity and skin depth, respectively.

Therefore, an ideal electromagnetic-thermal analysis engine should couple the electrical and thermal properties of the materials at each time step. Since the rate of change of thermal properties of the materials is much slower than that of the driving electromagnetic field, the maximum time step for TLM is much smaller than that of the thermal FDTD. As a result, coupling the two analyses at each TLM time step is neither necessary nor practical. In fact, it is sufficient to have a very loosely coupled algorithm that schedules the TLM and thermal analyses to be executed alternatively. It is not necessary to switch over to another engine as long as the change in material properties remains below some pre-determined threshold values.

We have coupled the generalized SCN TLM modeling procedure with a FDTD thermal engine based on the formulation given by equations 1–16. Switching between these two engines is controlled by two parameters, NUMBER_TLM_ITS and NUMBER_THERMAL_ITS. During the TLM simulation cycle, the average energy dissipated in the structure is computed. The dissipated energy includes both dielectric loss and metallic loss. For dielectric loss, the loss in each cell of discretization is stored in a three-dimensional array; for metallic loss, the loss on the metal surfaces is stored in a number of two-dimensional arrays. These arrays are passed to the thermal engine at the beginning of the thermal computation cycle. The thermal engine computes the temperature change based on the input energy distribution as well as energy losses due to radiation. At the end of the thermal cycles, new values for the dielectric constants and the conductivity are computed based on the temperature of the materials. The TLM-thermal cycles are repeated until the temperature of interest reaches a steady state. Since average power is used to evaluate the temperature change in the structure, the TLM cycle must have sufficient time steps for the integration process to compute the average power flow into the structure.

V. Numerical Results

Figures 1 and 2 show the power and temperature distributions in a cuboid volume ($8\times8\times4\ \Delta l^3$, where Δl = 5.375mm) of polyvinyl chloride (PVC) inside a cavity during a coupled analysis. The cavity is excited with the TE_{110} mode field distribution. Power dissipated in the PVC region is obtained by a volume-integration over the PVC region; this integration is performed automatically by our simulation engine. The equivalent heating rate can be computed as:

$$\frac{\Delta T}{\Delta t} = \frac{P_{diss\ in\ PVC}}{c_{PVC} \cdot mass_{PVC}} \tag{17}$$

where C_{PVC} (1.05 KJ / Kg^oK) is the specific heat constant of PVC. The power density distribution in Figure 1 yields a total dissipated power of 2W (average of 0.0078W per cell) in the PVC region. This yields an equivalent heat rate of 0.0345 ^oK/s. This value agrees well with the slope of the graph in Figure 2b, which is 0.0325^oK/s.

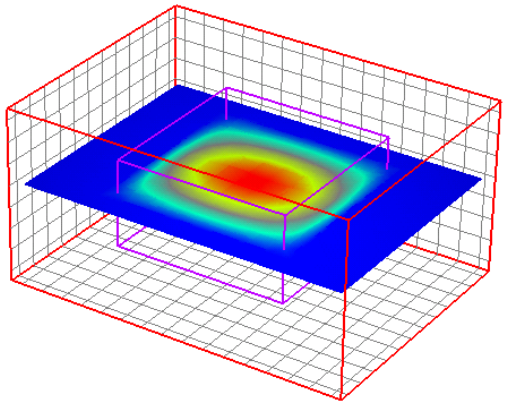

(a) 3D color representation

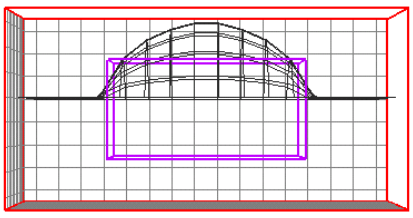

(b) 2D wire mesh representation

Figure 1: TE_{110} mode power density distribution in a PVC (ε_r=3.5, σ=2.e-6 S/m) loaded cavity. In the 3D color representation, red (center) and deep blue (background) colors are corresponding to 0.0156-W/cell (100 KW/m^3) and 0-W/cell, respectively. The 2D wire mesh representation gives the same information in another perspective.

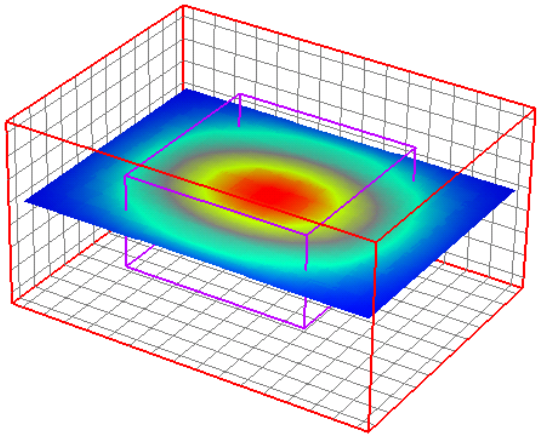

(a) 3D color representation

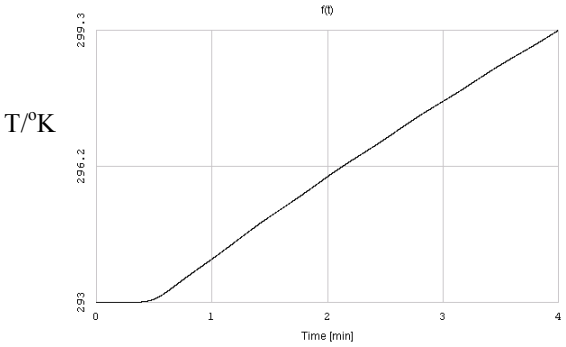

(b) Temperature increase in the center of the PVC block

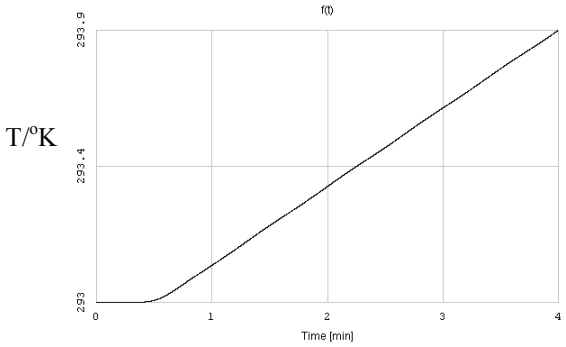

(c) Temperature increase in the air around the PVC block

Figure 2: Temperature distribution in the PVC loaded cavity. (a) Red (center) and deep blue (background) color are corresponding to 299.3^oK and 293^oK, respectively. The temperature evolution in the PVC block and in the air are shown in (b) and (c). The total power dissipated in the PVC region is 2-W, which is equivalent to a 0.035^oK /s heating rate.

VI. Conclusion

A loosely coupled hybrid TLM-thermal simulation program has been developed. The algorithm predicts the temperature rise and distribution inside guiding and resonant microwave structures and accounts for both metallic and dielectric material losses inside the structure. Transient heat conduction, convection and radiation transfer are taken into account. The program allows microwave engineers to couple electromagnetic simulations with thermal analysis in the time domain, thus making it possible to analyze structures with temperature dependent materials more accurately. Furthermore, the coupling is done loosely to avoid unnecessary computational overhead. Applications range from microwave heating and processing of materials to the evaluation of transient thermal stress and power handling capability of electromagnetic structures.

VII. References

[1] P.B. Johns, *A Symmetrical Condensed Node for the TLM Method*, IEEE Trans. Microwave Theory and Tech. vol. MTT-35, no. 4, pp. 370-377, April 1987.

[2] Wei Liu, Poman P.M. So and W.J.R. Hoefer, *Hybrid Modeling of Thermal Behavior of Metallic and Dielectric Objects Exposed to Waveguide Cavity Fields*, ACES, March 2001.

[3] J. Haala, W. Wiesbeck, *Modeling Microwave and Hybrid Heating using FDTD*, ACES, Volume 2, 2000.

[4] Viennet, C., So, P.P.M., and Hoefer, W.J.R., *Modeling of Transient Thermal Behavior of Discontinuities in Rectangular Waveguides*, in 29th European Microwave Conference Dig., pp. 199-202, Munich, Germany, October 5-7, 1999

[5] David M. Pozar, *Microwave Engineering*, Second Edition, John Wiley & Sons, Inc. 1998.